PERGAMON

International Journal of Multiphase Flow 27 (2001) 107–118

International Journal of Multiphase Flow

www.elsevier.com/locate/ijmulflow

Simulations of fluidization of cylindrical multiparticles in a three-dimensional space

Dewei Qi

Department of Paper and Printing Science and Engineering, College of Applied Science and Engineering, Western Michigan University, Kalamazoo, MI 49008, USA

Received 11 February 1999; received in revised form 31 December 1999

Abstract

The simulations of sedimentation of cylindrical particles falling against gravity are performed using a lattice Boltzmann method. The calculations of three-dimensional translation and rotation of cylinders are carried out. Cylindrical particle behavior is dominated by inertia effects associated with wakes. One cylindrical particle may be sucked in a strong wake behind other cylinder to form an inverted 'T' cluster. The long bodies of the cylinders turn horizontal dominantly due to a force couple generated by a high pressure at a stagnation point. These simulation results are well consistent with the experimental results of three-dimensional cylindrical and disk particles. It is demonstrated that the lattice Boltzmann method can handle cylindrical particles in a three-dimensional space correctly. © 2000 Elsevier Science Ltd. All rights reserved.

Keywords: Lattice Boltzmann simulation; Non-spherical particles; Suspensions; Sedimentary flows

1. Introduction

Solid particles in flows have extensive applications in various industries, such as food process, dyes, paints, proteins, photographic emulsion, ceramics, printing and papermaking. Some colloidal particles are spherical; other are non-spherical and may have very complex shapes. For example, the shape of calcium carbonate extensively used in the coating industry may be rhombohedral or cylindrical.

E-mail address: dewei.qi@wmich.edu (D. Qi).

PII: S0301-9322(00)00008-2

Although there are comprehensive studies on the behavior of spherical particle suspensions (Brady and Bossis, 1988; Happel and Pfeffer, 1960; Feng et al., 1994), very few studies on the properties of non-spherical suspensions have been reported. The non-spherical particles in finite-Reynolds number flows are difficult to model due to the lack of effective mathematical and simulation methods to handle the interactions between the fluid and the complex geometry of the particles.

The first experimental fluidization of cylinders and disks were reported by Joseph et al. (1987). A narrow channel was used to restrict one layer cylinders to be fluidized under gravity. Three-dimensional rotations were allowed for each cylinder in their experiments. They found that the behavior of cylindrical particles is quit different from that of spherical particles. The long bodies of cylindrical particles are dominantly perpendicular to the stream lines of flows. A high pressure at the point of stagnation gives rise to a couple causing the body to turn broadside. There are very strong wakes behind cylinders. One cylinder may be sucked into the wakes of other cylinder to form an inverted 'T' cluster, which is relatively stable for a while. After the cylinder is sucked into the wake of the other cylinder, the strength of the wake may be reduced, and the inverted 'T' cluster may be melt. The formation of inverted 'T' clusters is a feature of cylindrical suspensions. They also observed some doublet and triplet clusters formed by two or more cylinders floating broadside. More information can be found in the article by Joseph et al. (1987).

In a previous paper (Qi, 2000), the simulations of the fluidization of two-dimensional rectangular multi-particles falling against gravity were reported. It was shown that the lattice Boltzmann method has a capacity to deal with non-spherical particles in a two-dimensional space. The same method will be extended to deal with three-dimensional cylindrical particles in this paper. The calculations of three-dimensional translations and rotations of cylinders are carried out in this simulation and results will be reported. The purpose of this paper is to demonstrate that the lattice Boltzmann method can handle three-dimensional cylindrical multi-particles correctly.

2. Lattice Boltzmann simulation

The lattice Boltzmann method (Wolfram, 1986; D'humieres et al., 1986; D'humieres and Lallemand, 1987; Frisch et al., 1987; McNamara and Zanetti, 1988, Qian et al., 1992; Dahlburg et al., 1987) has been used to simulate non-spherical particles (Ladd, 1994a, 1994b; Koch and Ladd, 1997; Aidun et al., 1998; Aidun and Qi, 1998, Qi, 1997a, 1997b, 1999, 2000) in finite Reynolds number flows. In this method, the simulation domain is divided into a discrete cubic lattice. A distribution function of fluid density in the lattice nodes is used to represent fluid particles. A two speed model of LB simulation is used in this work. The fluid particles of type one move along the axes with speed of $\mathbf{e}_1 = 1$ and the fluid particles of type 2 moves along the diagonal directions with a speed of $\mathbf{e}_2 = \sqrt{3}$. Thus, each node has six nearest neighbors and eight next-nearest neighbors connected by a total of 14 links. The vectors $\mathbf{e}_{\sigma i}$ representing both lattice spacing and fluid particle velocities in the model are listed in Table 1 for the three-dimensional case.

The lattice Boltzmann (LB) equation with a single relaxation time is given by

$$f_{\sigma i}(\mathbf{x}+\mathbf{e}_{\sigma i}, t+1)-f_{\sigma i}(\mathbf{x}, t)=-\frac{1}{\tau}\Big[f_{\sigma i}(\mathbf{x}, t)-f^{(0)}_{\sigma i}(\mathbf{x}, t)\Big], \tag{2.1}$$

where $f_{\sigma i}(\mathbf{x}, t)$ is the fluid particle distribution function, $f^{(0)}_{\sigma i}(\mathbf{x}, t)$ is the equilibrium distribution function, τ is the single relaxation time. The kinematic viscosity ν is related to τ by $\nu=(2\tau-1)/6$. In the simulations, $f^{(0)}_{\sigma i}(\mathbf{x}, t)$ is taken

$$f^{(0)}_{\sigma i}(\mathbf{x}, t)=A_\sigma+B_\sigma(\mathbf{e}_{\sigma i}\cdot\mathbf{u})+C_\sigma(\mathbf{e}_{\sigma i}\cdot\mathbf{u})^2+D_\sigma u^2, \tag{2.2}$$

where $\sigma=1$ corresponds to the fluid particles moving to the near-neighbors along axial directions; $\sigma=2$ corresponds to the fluid particles moving to their second-near neighbors along diagonal directions; $\sigma=0$ and $i=0$ correspond to the fluid particles at rest; $\mathbf{u}$ is the mean velocity of fluid particles at a node. The coefficients in Eq. (2.2) are

$$A_1=\frac{1}{9}\rho_{\mathrm{f}},\quad B_1=\frac{1}{3}\rho_{\mathrm{f}}\quad C_1=\frac{1}{2}\rho_{\mathrm{f}}$$

$$D_1=-\frac{1}{6}\rho_{\mathrm{f}},\quad A_2=\frac{1}{72}\rho_{\mathrm{f}},\quad B_2=\frac{1}{24}\rho_{\mathrm{f}}$$

$$C_2=\frac{1}{16}\rho_{\mathrm{f}},\quad D_2=-\frac{1}{48}\rho_{\mathrm{f}},\quad A_0=\frac{2}{9}\rho_{\mathrm{f}}$$

$$D_0=-\frac{1}{6}\rho_{\mathrm{f}} \tag{2.3}$$

When solid particles are suspended in the fluid, the fluid flows may hit the surface boundary of solid particles. Ladd's (1994a) pioneer work for a moving boundary condition, in terms of a

Table 1
Spacing and fluid particle velocity vectors in cubic lattice in three-dimension

σ	i	$\mathbf{e}_{\sigma ix}$	$\mathbf{e}_{\sigma iy}$	$\mathbf{e}_{\sigma iz}$	$\lvert\mathbf{e}_{\sigma i}\rvert$
1	1	1	0	0	1
1	2	−1	0	0	1
1	3	0	1	0	1
1	4	0	−1	0	1
1	5	0	0	1	1
1	6	0	0	−1	1
2	1	1	1	1	$3^{1/2}$
2	2	−1	−1	−1	$3^{1/2}$
2	3	−1	1	1	$3^{1/2}$
2	4	1	−1	−1	$3^{1/2}$
2	5	−1	−1	1	$3^{1/2}$
2	6	1	1	−1	$3^{1/2}$
2	7	1	−1	1	$3^{1/2}$
2	8	−1	1	−1	$3^{1/2}$

collision rule, in the LB scheme makes simulation of a suspension in finite-Reynolds-number flows possible. This boundary condition is expressed by

$$f_{\sigma i'}(\mathbf{x}, t+1) = f_{\sigma i}(\mathbf{x}, t_+) - 2B_\sigma(\mathbf{e}_{\sigma i} \cdot \mathbf{V}_b), \tag{2.4}$$

where $\mathbf{x}$ is the position of the node adjacent to the solid-surface with velocity $\mathbf{V}_b$ t_+ is the post collision time which is the same as the definition by Ladd (1994a), i' denotes the reflected direction, and i the incident direction. The above rule is applied to the boundary nodes in both sides of the solid-surface. As a result, a no-slip boundary condition for moving solid particles is imposed by the collision rule in such a way that the fluid mass is conserved at each time step by allowing exchange of population of fluid at the boundary nodes adjacent to both sides of the solid-surface. The hydrodynamic force exerted on the solid particle at the boundary node is

$$F\left(\mathbf{x} + \frac{1}{2}\mathbf{e}_{\sigma i}\right) = 2\mathbf{e}_{\sigma i}\left(f_{\sigma i}(\mathbf{x}, t_+) - B_\sigma(\mathbf{V}_b \cdot \mathbf{e}_{\sigma i})\right) \tag{2.5}$$

where $\mathbf{V}_b = \mathbf{V}_0 + \boldsymbol{\Omega} \times \mathbf{x}_b$, $\mathbf{V}_0$ is the velocity of the center of mass; $\mathbf{V}_b$ is the velocity of solid–fluid interface at the node; Ω is the angular velocity of the solid particle; $\mathbf{x}_b = \mathbf{x} + \frac{1}{2}\mathbf{e}_{\sigma i} - \mathbf{R}$, $\mathbf{R}$ is the center of the corresponding solid particle. The total force F_T and torques T_T on the solid particles are obtained by

$$F_\mathrm{T} = \sum F\left(\mathbf{x} + \frac{1}{2}\mathbf{e}_{\sigma i}\right) \tag{2.6}$$

$$T_\mathrm{T} = \sum\left(\mathbf{x} + \frac{1}{2}\mathbf{e}_{\sigma i} - \mathbf{R}\right) \times F\left(\mathbf{x} + \frac{1}{2}\mathbf{e}_{\sigma i}\right) \tag{2.7}$$

The summation is over all the boundary nodes in the fluid region associated with a particular solid particle.

In the lattice Boltzmann method, the nodes are fixed and the solid particles move over the (nodes) grids. Whenever a node relatively crosses the fluid–solid interface and enters the solid region, the momentum of the flow at the boundary node may exert a force on the solid particle. The force F_I (Aidun et al., 1998; Qi, 1999) at the node is

$$F_\mathrm{I}(\mathbf{x}, t) = \rho_\mathrm{f}(\mathbf{x}, t)\mathbf{u}(\mathbf{x}, t) \tag{2.8}$$

where ρ_f is the density of the fluid at the node. Similarly, whenever a node relatively crosses the solid–fluid interface and leave the solid region, the flow in the node should add a force F_O on the solid particle, i.e.

$$F_\mathrm{O}(\mathbf{x}, t) = -\rho_\mathrm{f}(\mathbf{x}, t)\mathbf{u}(\mathbf{x}, t) \tag{2.9}$$

The present approach still allows fluid to enter the inside of solid to conserve the total mass of fluid at each time step. The conservation of fluid mass guarantees the recovery of the Navier–Stokes equations from LB method. This is particularly important for multiparticles. If the fluid mass in the system is not conserved due to the existence of a single solid particle, this unconservation of fluid mass will be accumulated due to the existence of multiparticles.

Therefore, the function of the fluid within solid region is to ensure that the Navier–Stokes equations are valid in the fluid region.

A proper calculation of rotation of non-spherical particles in a three-dimensional space is necessary in simulations. The details about the calculation have been described in Qi (1997a, 1997b).

The translations of the mass center of each particle are updated at each Newtonian dynamic time step by using a so-called 'velocity-Verlet' scheme (Swope et al., 1982). The scheme is written as:

$$\mathbf{R}(t+\delta t) = \mathbf{R}(t) + \delta t \mathbf{V}_0(t) + \frac{1}{2}\delta t^2 \mathbf{F}(t)/M \tag{2.10}$$

$$\mathbf{V}_0(t+\delta t) = \mathbf{V}_0(t) + \frac{1}{2}\delta t \mathbf{F}(t)/M + \mathbf{F}(t+\delta t)/M \tag{2.11}$$

where $\mathbf{R}$ is the position of the mass center of a solid particle, $\mathbf{F}$ is the total force on the solid particle, and M is the mass of the solid particle.

The reliability of the LB simulation of suspensions at finite Reynolds numbers has been evaluated by comparing LB simulation results with both finite-element and experimental results (Qi, 1999).

3. Fluidization of cylindrical particles

3.1. Simulations

The size of the simulation box is $140 \times 30 \times 150$ initially. Four walls are fixed at $x = 0$, $x = 140$, $y = 0$ and $y = 30$, respectively. The length, l, of a cylinder is 24 and the diameter, D, is 12. The cross section of the cylinder is shown in Fig. 1 and the ends of the cylinder are rounded by an arc of radius 1.5. The cylinder is formed by revolving the cross section around z–z axis.

The size of the channel used allows the cylinders to rotate in the three-dimensional space. An array of 16 cylinders is initially located in a regular order in the channel and the Euler angles ϕ, θ, and ψ for all the cylinders are set to 45° 90° and 0°, respectively, as shown in the leftmost image in the top row of Fig. 2. The fluid velocity at the bottom boundary is set to zero and this boundary is always 42.84 ahead the bottom particle. The fluid distribution at the bottom nodes is reset by $f_{\sigma i}^{(0)}(\mathbf{x}, t) = A_\sigma$ at $\mathbf{u} = 0$ at each time step. Whenever the bottom particle move over one lattice distance, a layer of fluid is added at the bottom nodes with the same condition. The stress at the top boundary is set to zero and the boundary is always 32.17 behind the top particle. The fluid particles in the vertical links and diagonal links are copied from the top nodes to the next-top nodes at each time step. Whenever the top particle moves over one lattice unit, the top fluid is removed. Therefore, the simulation box is expanded in the gravity direction during simulation due to relative movement among the particles and the boundary conditions used in this work. The final global particle Reynolds number is 16.92,

which is defined by $Re = V_f * l/\nu$, where V_f is the final global velocity of particles. The corresponding solid density is 1.035. It has been assumed that the fluid density is 1.

Fig. 3 shows the global average velocity of all particles in the settling direction. The particle velocity increase during initial settling and then become stable with a small oscillation.

3.2. Orientation of cylinderrs

The simulations provide all dynamical information, such as the positions and velocities of solid particles and the velocities of flows. Therefore, the macrostructure of particles can be easily analyzed from this information.

The cylinders collectively turn horizontal quickly as shown in the top row of Fig. 2. Then their positions and orientations become more random due to strong interactions between the cylinders and the flows. However, the longer bodies of the cylinders are dominantly oriented in the horizontal direction on an ensemble average. The cylinders in a vertical direction are not stable, they may turn to the horizontal direction. Stable doublets formed by two cylinders floating broadside are observed, as shown in Fig. 2. The polar angle, θ, can be used to characterize the orientation and measure the degree of a cylinder perpendicular to the vertical direction. An angular distribution function (ADF) is adopted to statistically evaluate the orientation of a random suspension of cylinders. The ADF is defined as a probability of finding a single cylinder with a given polar angle θ per unit angle and written as

$$f(\theta) = \frac{1}{n}\sum_i \langle \delta(\theta) - \delta(\theta_i) \rangle \tag{3.1}$$

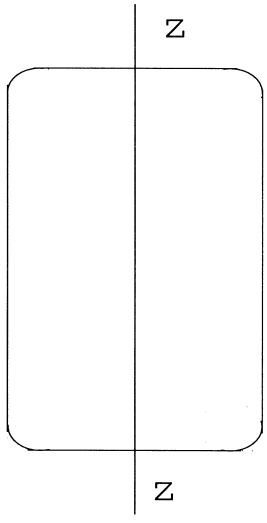

Fig. 1. The ends of a cylinder are rounded by an arc and the cylincer is formed by revolving the cross section around z–z axis.

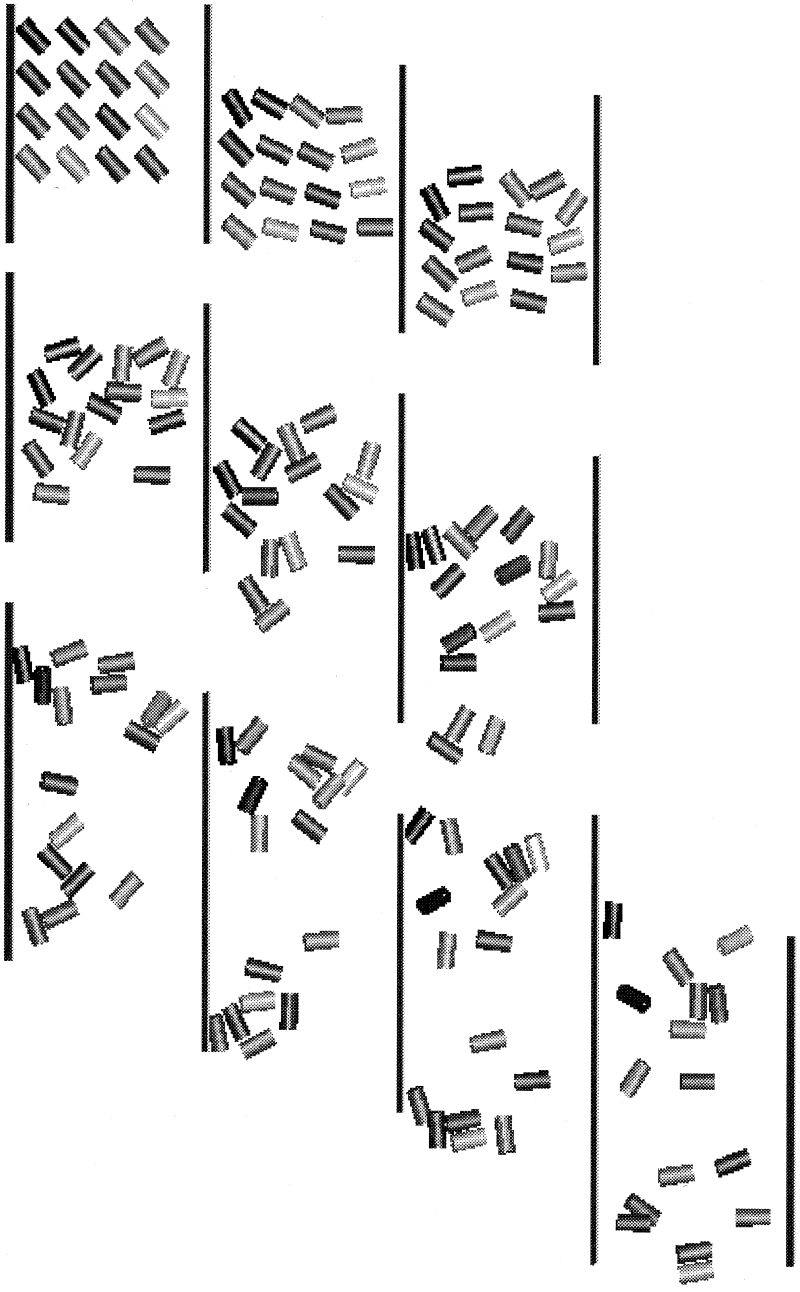

Fig. 2. Snap shots of sedimentation of 16 three-dimensional cylinders with final global $Re = 16.92$. The images in the first row from the left to right correspond to a time order at $t = 0$, 5000 and 10,000, those in the second row correspond to $t = 15{,}000$, 20,000 and 25,000, and those in the third row corresponding to $t = 30{,}000$, 35,000, 40,000, 45,000.

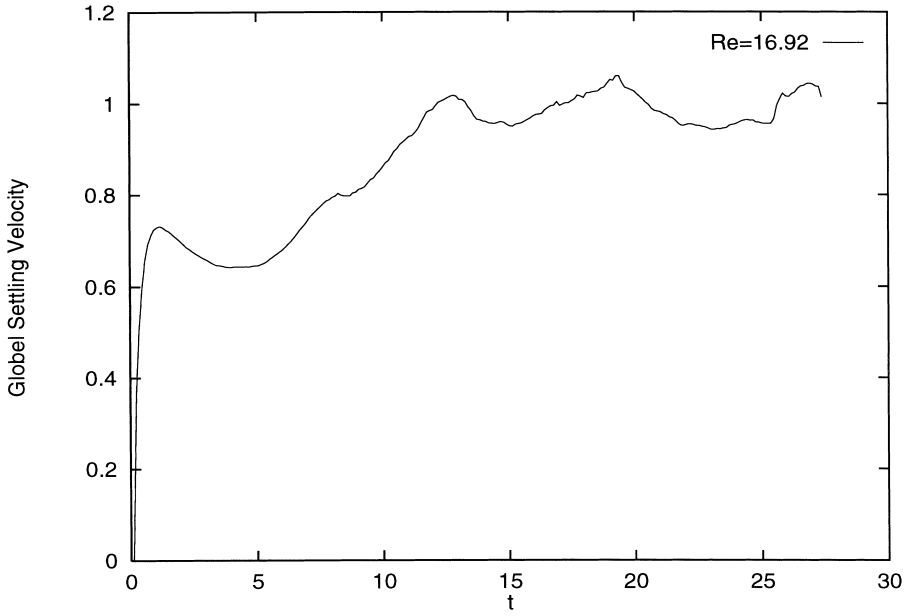

Fig. 3. The global velocity in the settling direction as a function of time for the cases with final $Re = 16.92$. The

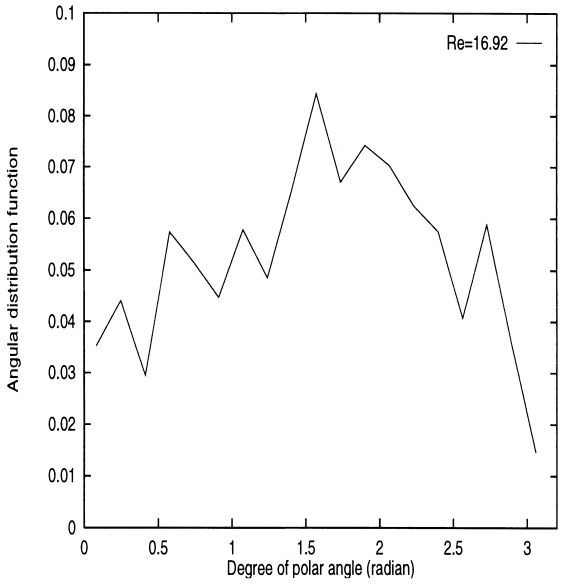

Fig. 4. The angular distribution function (normalized to 1) is shown at final particle Reynolds number $Re = 16.92$. Since the settling direction is in the z-direction, the polar angle $\theta = \pi/2$ corresponds to the horizontal direction.

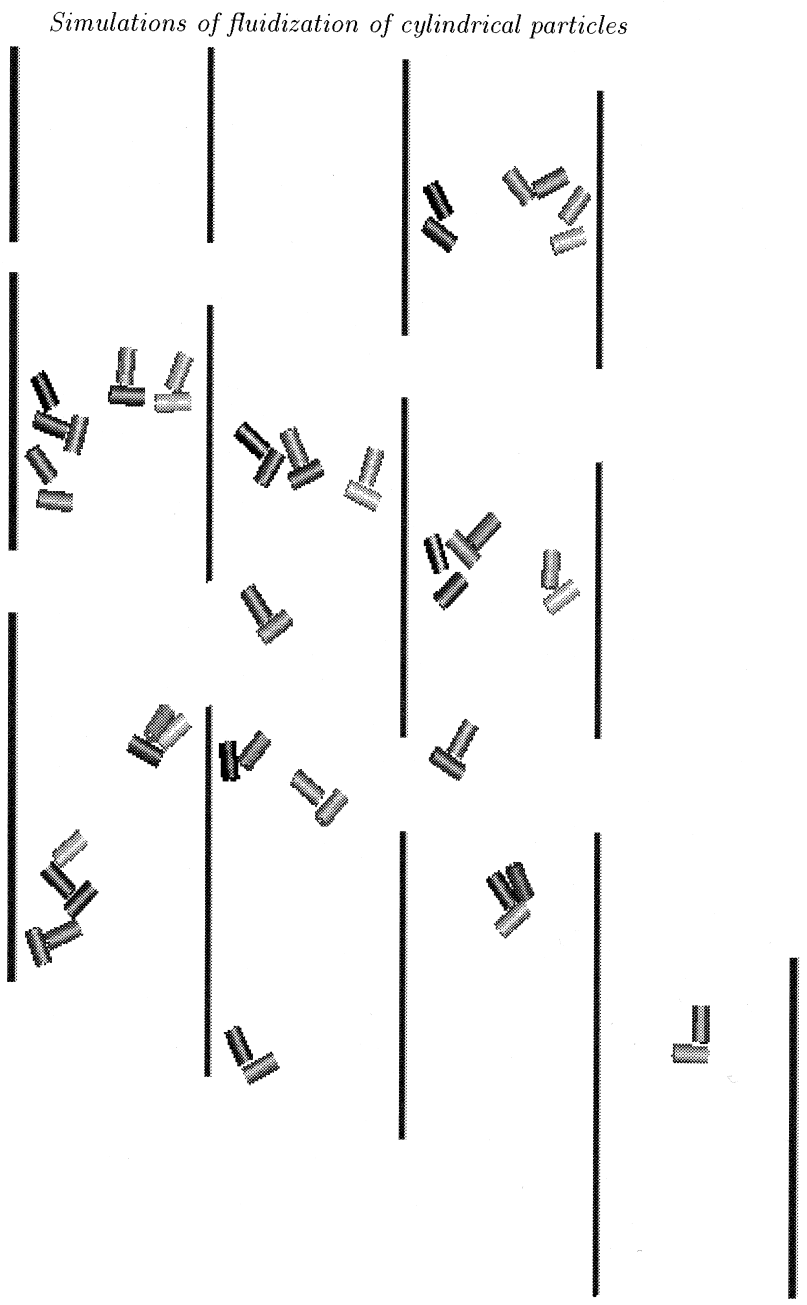

Fig. 5. The inverted T clusters formed by two cylinders and some doublets are shown. The configurations are the same as those in Fig. 2 except that other type of clusters are intentionally suppressed to show the inverted T clusters and some doublets more clearly.

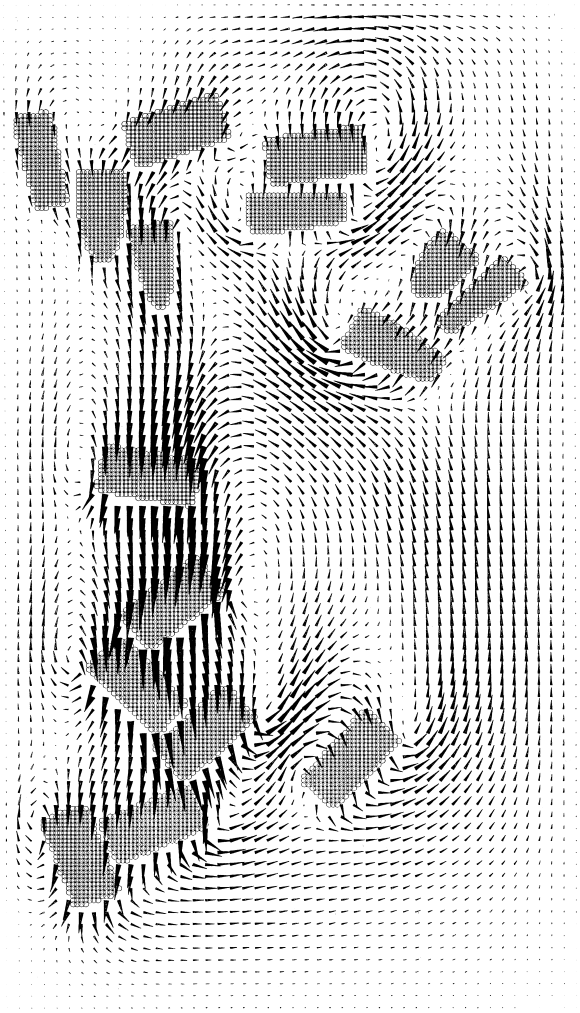

Fig. 6. projection of velocity on x–z plane at $y = H/2$ is shown, where H is the thickness of the simulation box. The section is the same as the rightmost images in the third row of Fig. 2 corresponding to $t = 30{,}000$. A complex velocity field with wakes is observed. The shaded circles represent the cross sections of cylinders. The values of the arrows representing the fluid velocities are scaled in an arbitrary unit.

where δ is Dirac delta function, $\langle\cdot\rangle$ stands for an ensemble average, and n is the total number of the cylinders.

The ensemble average of the angles is carried out for 100 configurations, each 200 time-step apart. The results for the periods from $t = 10{,}000$ to $t = 30{,}000$ are shown in Fig. 4.

It is clearly observed that the long bodies of cylinders broadside are always dominated during settling as shown in Figs. 2 and 4. The probability is much larger at $\theta = 90^\circ$ than at other angles, indicating that the horizontal angle ordering is a feature of slender body in sedimenting flows. A high pressure is produced in the front side of a particle and a wake is

generated on the back. The high pressure at the stagnation points gives rise to a couple causing the body to turn broadside. This has been explained clearly by Joseph et al. (1987) and Huang et al. (1994).

3.3. Structure of clusters

One cylindrical particle may be sucked in strong wakes behind other cylinder to form an inverted 'T' cluster, this is a drafting and kissing process. The inverted 'T' cluster may be stable for a short period. After sucking a cylinder, the strength of the wake may be reduced, and the inverted 'T' cluster is melt or dispersed. The inverted 'T' clusters, each formed by two particles, are shown in Fig. 5. In these figures, the inverted 'T' clusters and some doublets are shown, other clusters are intentionally suppressed in order to see them clearly.

Drafting, kissing and melting may be used to characterize the behavior of aggregation and dispersion due to multi-particle interaction governed by inertia wake effects. These simulation results are well consistent with the experimental work of Joseph et al. (1987) who found the similar behavior of non-spherical particles.

A complex velocity field in the simulation box at $t = 30{,}000$ is shown in Fig. 6. As expected, there are many wakes behind cylinders.

4. Conclusions

Fluidization of 16 cylindrical particles falling under gravity has been simulated by using the lattice Boltzmann method. The calculations of three-dimensional translations and rotations of cylinders are included in the simulation. An angular distribution function is used to describe the orientation of the cylinders and the results show that the long bodies of cylinders turn horizontal dominantly during falling. Relative stable doublets formed by two cylinders floating broadside are observed.

One cylinder may be sucked into a strong wake behind other cylinder to form an inverted 'T' cluster. Drafting, kissing and melting may be used to describe the interaction between the cylinders. These behavior dominated by the effects of inertia are well consistent with the experimental works of Joseph. It has been demonstrated that the LB method has a capacity to handle non-spherical particles in the three-dimensional space. Valuable discussions with Professor D. Joseph, A.J.C. Ladd and D. Koch are greatly appreciated.

References

Aidun, C.K., Lu, Y., Ding, E., 1998. Direct analysis of particulate suspensions with inertia using the discrete Boltzmann equation. J. Fluid Mech 373, 287–311.

Aidun, C.K., Qi, D., 1998. A new method for analysis of the fluid interaction with a deformable membrane. J. Stat. Phys 90, 145–158.

Brady, J.F., Bossis, G., 1988. Stokesian dynamics. Ann. Rev. Fluid Mech 20, 111–157.

Dahlburg, J.P., Montgomery, D., Doolen, G., 1987. Noise and compressibility in lattice-gas fluids. Phys. Rev. A 36, 2471–2475.

d'Humieres, D., Lallemand, P., Frisch, U., 1986. Lattice gas model for 3D hydrodynamics. Europhys. Lett 2, 291–297.

D'Humieres, D., Lallemand, P., 1987. Numerical simulation of hydrodynamics with lattice gas automata in two dimension. Complex Systems 1, 599–632.

Feng, J., Hu, H.H., Joseph, D.D., 1994. Direct simulation of initial value problems for the motion of solid bodies in a Newtonian fluid. Part 1: Sedimentation. J. Fluid Mech 261, 95–134.

Frisch, U., D'Humieres, D., Hasslacher, B., Lallemand, P., Pomeau, Y., Rivet, J.-P., 1987. Lattice gas hydrodynamics in two and three dimensions. Complex Systems 1, 649–707.

Happel, J., Pfeffer, R., 1960. The motion of two spheres following each other in a viscous fluid. Al.Ch.E. Journal 6 (1), 129–133.

Huang, P., Feng, J., Joseph, D., 1994. The turning couples on an elliptic particle settling in a vertical channel. J. Fluid Mech 271, 1–16.

Joseph, D.D., Fortes, A.F., Lundgreen, T.S., Singh, P., 1987. Nonlinear mechanics of fluidization of beds of spheres cylinders and disks in water. In: Papanicolau, G. (Ed.), Advances in Multiphase Flow and Related Problems. SIAM, Philadelphia, PA, pp. 101–122.

Koch, D.L., Ladd, A.J.C., 1997. Moderate Reynolds number flows through periodic and random arrays of aligned cylinders. J. Fluid Mech 349, 31–66.

Ladd, A.J.C., 1994a. Numerical simulations of particulate suspensions via a discretized Boltzmann equation. Part 1: Theoretical foundation. J. Fluid Mech 271, 285–309.

Ladd, A.J.C., 1994b. Numerical simulations of particulate suspensions via a discretized Boltzmann equation. Part 2: Numerical results. J. Fluid Mech 271, 311–339.

McNamara, G., Zanetti, G., 1988. Use of Boltzmann equation to simulate lattice-gas automata. Phys. Rev. Lett 61, 2332–2335.

Qian, Y., dHumieres, D., Lallemand, P., 1992. Lattice BGK models for Navier–Stokes equation. Europhys. Lett 17, 479–484.

Qi, D.W., 1997a. Non-spheric colloidal suspensions in three-dimensional space. Int. J. Mod. Phys 8, 985–997.

Qi, D.W., 1997b. Computer simulation of coating suspensions. In: Proceedings, Tappi Advanced Coating Fundamental Symposium, May, Philadelphia, PA, 201–211.

Qi, D.W., 1999. Lattice Boltzmann simulations of particles in No-zero-Reynolds-number flows. J. Fluid Mech 385, 41–62.

Qi, D.W., 2000. Lattice Boltzmann simulations of fluidization of rectangular particles. Int. J. Multiphase Fluid 26, 421–433.

Swope, W.C., Anderson, H.C., Berens, P.H., Wilson, K.R., 1982. A computer simulation method for the calculation of equilibrium constants for formation of physical clusters of molecules: application to small water clusters. J. Chem. Phys 76, 637–649.

Wolfram, S., 1986. Cellular automaton fluids. Part 1: Basic theory. J. Stat. Phys 45, 471–526.